Cancer Letters 372 (2016) 118–127

Contents lists available at ScienceDirect

Cancer Letters

journal homepage: www.elsevier.com/locate/canlet

Original Articles

MMGZ01, an anti-DLL4 monoclonal antibody, promotes nonfunctional vessels and inhibits breast tumor growth

Zhuobin Xu [1], Zegen Wang [1,2], Xuelian Jia, Luxuan Wang, Zhiguo Chen [3], Shijing Wang, Min Wang *, Juan Zhang **, Min Wu ***

State Key Laboratory of Natural Medicines, School of Life Science and Technology, China Pharmaceutical University, Nanjing 210009, China

ARTICLE INFO

Article history:
Received 6 November 2015
Received in revised form 15 December 2015
Accepted 16 December 2015

Keywords:
DLL4 monoclonal antibody
Notch
Breast cancer
Nonfunctional vessels
Antitumor
Angiogenesis

ABSTRACT

Increasing evidence suggests that DLL4 (Delta-like 4)-Notch signaling plays a critical role in cell fate determination and differentiation in tissues. Blocking DLL4-Notch signaling results in inhibition of tumor growth, which is associated with increased nonfunctional vessels and poor perfusion in the tumor. We successfully generated a human DLL4 monoclonal antibody MMGZ01 that binds specifically to DLL4 to disrupt the interaction between DLL4 and Notch1. MMGZ01 showed high affinity to DLL4 to inhibit the DLL4-mediated human umbilical vein endothelial cell (HUVEC) phenotype. Furthermore, MMGZ01 stimulated HUVEC vessel sprouting and tubule formation in vitro. In addition, MMGZ01 had a pronounced effect in promoting immature vessels and reduced breast cancer cell growth in vivo. Finally, MMGZ01 treatment inhibited the proliferation of breast cancer cells, induced tumor cell apoptosis, suppressed mammosphere formation, decreased $CD44^{+}/CD24^{-}$ cell population, and reduced epithelial mesenchymal transition (EMT). These findings suggest that antagonism of the DLL4-Notch signaling pathway might provide a potential therapeutic approach for breast cancer treatment.

Introduction

Breast carcinoma leads to the highest rate of cancer death and is associated with an extremely poor clinical prognosis among women [1–3]. Similarly to many other human pathologies, breast cancer is induced by cumulative genetic, epigenetic, somatic, and endocrine aberrations. Although adjuvant therapies such as chemotherapy and endocrine therapies were widely developed in early breast cancer treatment, the recurrence rate remains largely unchanged [2,4]. Chemoresistance remains an urgent issue in the clinical therapy of breast cancer [5].

DLL4 (Delta-like 4), a component of the Notch signaling pathway, is confined dramatically to the vascular endothelium and was first reported by the Stark group in 2000 [6]. DLL4 is a single pass transmembrane protein, containing an extracellular region consisting of a cysteine-rich DSL motif and EGF motifs, a trans-membrane domain and an intracellular domain [7,8]. DLL4-Notch interactions between adjacent cells trigger two successive proteolytic cleavages within the extracellular region of Notch receptors; these cleavages release the intracellular fragment of Notch, which translocates to the nucleus, mediating the transcription of downstream target genes, such as the hairy/enhancer of split (Hes) and Hes-related (Hey) families [9–11]. DLL4-Notch signaling is apparently required for endothelial cells in response to angiogenic signals. DLL4 blocks the formation of sprouting endothelial tip cells and promotes the formation of stalk cells to induce vessel maturation [11]. Mice deficient in even a single DLL4 allele result in embryonic lethality with multiple severe vascular abnormalities, including arteriovenous malformations and embryonic vascular remodeling defects [12].

Over-expression of DLL4 and the activation of Notch signaling have been identified in several types of cancers, including breast cancer [13], T-ALL leukemia [14], glioma [15], pancreatic carcinoma [16], gastric cancer [17], and bladder cancer [18]. The blockade of DLL4-Notch signaling disrupts angiogenesis in an extraordinary manner by inducing hyperproliferation of nonfunctional tumor vessels that result in tumor growth inhibition in mouse models [19,20]. Yan et al. showed that inhibition of DLL4-Notch signaling by a soluble form of a DLL4 or anti-DLL4 monoclonal antibody could decrease tumor growth in bevacizumab-sensitive or -resistant tumors [20]. In addition to its role in regulating tumor vasculature, evidence suggests that aberrant Notch signaling is associated with the differentiation, proliferation, progression and survival of breast cancer

* Corresponding author. Tel.: +86 25 8327 1395; fax: +86 25 8327 1395.
E-mail address: minwang@cpu.edu.cn (M. Wang).
** Corresponding author. Tel.: +86 25 8327 1483; fax: +86 25 8327 1395.
E-mail address: juancpu@126.com (J. Zhang).
*** Corresponding author. Tel.: +86 138 5164 6797; fax: +86 25 8327 1395.
E-mail address: mickeywu2001@163.com (M. Wu).
[1] The authors Zhuobin Xu and Zegen Wang contributed equally to this work.
[2] Present address: Cyrus Tang Hematology Center, Soochow University, Suzhou, China.
[3] Present address: Department of Biotechnology and Environmental Science, Changsha University, Changsha, China.

http://dx.doi.org/10.1016/j.canlet.2015.12.025
0304-3835/

[5,21,22]. Jubb et al. reported that DLL4 is expressed in breast cancer associated endothelial cells, suggesting that tumor endothelial DLL4 expression is a significant prognostic factor of breast adenocarcinoma [13]. DLL4-Notch signaling has also been implicated in the regulation of the cancer stem cell (CSC) phenotype in several cancer types, which maintains tumor growth, promotes tumor metastasis and promotes resistance to many existing therapies [23,24]. The breast cancer stem-like cell phenotype, which is characterized by cell markers $CD44^+/CD24^-$, is demonstrated to correlate with upregulation of Notch expression [25,26]. Notch signaling inhibitors such as neutralizing antibodies of ligands or receptors and GSI have also been reported to inhibit tumor growth by reducing tumor-initiating cell frequency.

Herein, we developed a monoclonal antibody against DLL4 and evaluated the effects in deregulating angiogenesis and the potential antitumor efficacy of this antibody in breast cancer as a single agent or in combination with docetaxel.

Materials and methods

Cell culture

HUVECs were acquired from the American Type Culture Collection (ATCC). The human breast adenocarcinoma cell lines MCF-7 and MDA-MB-231 were obtained from the cell bank of the Chinese Academy of Sciences (Shanghai, China). The Sp2/0-Ag14 murine myeloma cells and HEK293 cells were preserved in our lab. All cells were cultured under recommended medium conditions and incubated in a humidified atmosphere with 5% CO_2 at 37 °C under standard cell culture techniques.

Antibody preparation and purification

Recombinant human delta-like 4 (rhDLL4) (50 μg) mixed with an equal volume of Quick Antibody™ (Kang Biquan Biotechnology Co., Beijing, China) adjuvant was injected intramuscularly into six-week-old female BALB/C mice (Yangzhou University Comparative Medicine Centre, Yangzhou, China) for first immunization. 3 weeks later, a booster immunization was conducted in the same way. Then an indirect ELISA assay was performed to measure the serum antibody titers 7 days later, and the mouse with the highest serum antibody titer was chosen for spleen donor. The donor mouse was sacrificed 3 days after a final immunization, and the immunized spleen cells were isolated. 5×10^8 spleen cells were fused with SP2/0 Ag-14 at the ratio of 5:1 in the presence of PEG(MW 1450) (Sigma-Aldrich, St. Louis/MO, USA) and added into 96-well plates. Hybridomas were selected in complete DMEM-20% FBS with 1 × HAT supplement (10 mM sodium hypoxanthanine, 40 μM aminopterin and 1.6 mM thymidine) for 7 days, and then selected in complete DMEM-20% FBS with 1 × HT supplement (10 mM sodium hypoxanthanine and 1.6 mM thymidine) for another 7 days [27]. After HT selection, the supernatants were collected and an indirect ELISA was performed to screen the positive hybridoma wells. Finally the stable hybridoma clones were selected after 3 cycles subcloning by limited dilution, and one positive hybridoma subclone named MMGZ01 was expanded in production medium.

Serum antibody titre measurement

ELISA plates were coated with 1 μg/mL of rhDLL4 at 4 °C overnight. After blocking for 2 h at 37 °C, different dilutions of immunized serum samples and negative serum samples were added to each well and incubated for 1 hour at 37 °C. After washing, HRP-goat anti-mouse IgG was added and incubated for 1 hour at 37 °C. Then, the peroxidase substrate was added and the OD_{450nm} with a reference OD_{630nm} of each well was measured.

Affinity measurement

The binding affinity of MMGZ01 to rhDLL4 was measured using a Biacore system (GE Healthcare, Sweden). A NTA sensor chip (GE Healthcare, Sweden) was activated with 0.5 mM $NiCl_2$ at 25 °C. Next, rhDLL4 carrying C-terminal histidine tag was captured when the target resonance unit (RU) density reached 200 followed by injection of different concentrations of MMGZ01 into running buffer (10 mM HEPES, 150 mM NaCl, 0.005% Surfactant P20, 3 mM EDTA at pH 7.4), which was filtered and degassed prior to use. At the same time, one flow cell of the sensor chip was left without immobilized with rhDLL4 to provide a reference surface, and the association rate constant was obtained. The dissociation rates were measured at a flow rate of 30 μL/min. Finally the sensorgrams at each concentration were evaluated with Bivalent analyte [28]. The equilibrium constant (KD) was calculated by kd/ka (association rate constant for ka and dissociation rate constant for kd).

Cell based DLL4 FACS binding assay and laser confocal fluorescence microscopy

The recombinant plasmid pEGFP-DLL4 (ECD) was constructed by cloning the extracellular fragment of DLL4 cDNA into the prokaryotic expression vector pEGFP which encodes a red-shifted variant of wild-type GFP [29]. To demonstrate the specificity of MMGZ01 in a cellular context, HEK293 cells were transiently transfected with the pEGFP-DLL4 eukaryotic recombinant plasmid. After 48 hours, 5×10^5 DLL4 (ECD) expressing HEK293 cells or DLL4 (ECD)-negative HEK293 cells were resuspended and incubated with/without 10 μg/mL MMGZ01 or the control DLL4 mouse mAb (Abcam, Cambridge, UK) for 1 hour. After washing, the cells were incubated with APC-conjugated goat anti-mouse IgG antibody (Miltenyi Biotec, Germany). Finally, an antibody binding assay was performed with the FACS Caliber (BD Biosciences, USA).

To further demonstrate the specificity of MMGZ01 to cell surface-expressed DLL4, confocal immunofluorescence microscopy of cells was performed. DLL4 (ECD) expressing HEK293 cells or DLL4 (ECD)-negative HEK293 cells were incubated with MMGZ01 or control DLL4 mouse mAb (Abcam, Cambridge, UK) at 4 °C overnight after being fixed and blocked. The binding properties of HEK293 expressing DLL4 (ECD) with MMGZ01 or control mouse anti-DLL4 antibody were visualized by APC-conjugated goat anti-mouse IgG antibody (Abcam, Cambridge, UK). Cell imaging was obtained with laser confocal fluorescence microscopy (FluoView™ FV1000, Olympus, Japan).

Protein extraction and Western blotting assay

HUVECs (2×10^5) were seeded into a 6-well plate that was pre-coated with rhDLL4 (1 μg/mL) for 4 hours at 37 °C and then treated with different concentration of MMGZ01 or vehicle control for 24 hours. The HUVECs were trypsinized and protein lysates were prepared in RIPA buffer (Beyotime, Shanghai, China) containing protease inhibitors for 0.5 hour. In the xenograft experiment, the collected tumor tissues were minced into small pieces and cell extracts were collected in RAPI buffer containing protease inhibitors for 1 hour [30]. Proteins were separated by SDS-PAGE and transferred onto PVDF membranes (Millipore, Billerica, USA). After blocking, the membranes were incubated with primary antibodies overnight and were then probed with corresponding HRP-conjugated antibodies. Bound antibodies were detected with ECL western blotting substrate (Millipore, Billerica, USA) and exposed by Bio-Rad ChemiDoc XRS.

HUVEC proliferation assay

96-well plates were coated with rhDLL4 (1 μg/mL) at 4 °C overnight. After washing, 4×10^3 HUVECs were seeded into the rhDLL4-coated wells to attach for 24 hours. Different concentrations of MMGZ01 and vehicle control were added immediately in triplicate. After incubation at 37 °C, 5% CO_2 for 72 hours, HUVEC proliferation was quantified by a MTT assay.

HUVEC tube formation assay

The effect of MMGZ01 on angiogenesis was evaluated in a tube formation assay. Growth factor reduced Matrigel (BD Biosciences, USA) (100 μL) was seeded into each well of a 96-well plate and allowed to polymerize at 37 °C. Then, 2.5×10^4 HUVECs mixed with 5 ng VEGF (Sino Biological Inc., Beijing, China) suspended in 100 μL ECM supplemented with 2% FBS were added into each well with vehicle control, 5 μg/mL bevacizumab, 5 or 10 μg/mL MMGZ01 and then incubated at 37 °C. After 4–16 hours cultivation, 50 μL of 6 μM calcein AM (Sigma-Aldrich, USA) solution was added to each well without aspirating the medium, and the plate was incubated for 15–30 min protected from light [31]. The calcein AM-labeled cultures were photographed with an OLYMPUS inverted microscope under 100-times magnification, and the quantity of endothelial tubes was counted with the Image-Pro-Plus program.

Vessel sprouting

HUVECs were suspended in culture medium containing 20% (w/v) carboxymethylcellulose (Sigma-Aldrich, USA). Then, HUVEC spheroids were generated by seeding approximately 1×10^3 HUVECs in a nonadherent round-bottom 96-well plate. After being cultured overnight, HUVECs formed a single spheroid per well with approximately 500 cells/spheroid. The suspending spheroids were embedded into collagen gels, as described previously [32,33]. Then, 500 μL of spheroid-containing gel was rapidly transferred into 24-well plates and allowed to polymerize for 30 minutes at 37 °C, and 100 μL of ECM basal medium mixed with 20 ng VEGF and vehicle control, 5 μg/mL bevacizumab, 5 or 10 μg/mL MMGZ01 was added on top of the gel [34]. After 48 hours incubation, the spheroids were stained with 50 μL of 20 μM calcein AM for 3 hours. Calcein-labeled spheroids were imaged by an OLYMPUS inverted microscope under 100-times magnification, and the sprouting vessels were recorded.

In vivo Matrigel plug angiogenesis assay

HUVEC spheroids were prepared as described earlier. After mixing Matrigel with HUVEC spheroids, the spheroid–Matrigel combination, which was mixed with VEGF-A and FGF-2 at a final concentration of 1000 ng/mL [35,36], was injected subcutane-

ously into the abdomen of 6-week-old female BALB/C nude mice (Yangzhou University Comparative Medicine Centre, Yangzhou, China). Randomly divided mice were treated every three days, beginning on day 2, with vehicle control, 1 mg/kg bevacizumab, 0.1 or 1 mg/kg MMGZ01. On day 21, the mice were sacrificed, and the Matrigel plugs were harvested and processed for immunofluorescence analysis.

Subcutaneous xenograft models

Six-week-old female nude mice (Yangzhou University Comparative Medicine Centre, Yangzhou, China) were used for all of the xenograft models. Tumor cells (5×10^6) were suspended in sterile PBS and implanted subcutaneously in the flank area of each mouse. To determine the effect of antibody on xenograft tumor growth, nude mice were randomly assigned to groups, and treatment started when the mean tumor volumes reached 100–150 mm^3. MDA-MB-231 tumors occured at about day 11 after implant, and treatment started at day 17. For MCF-7 model, the tumors occured around day 14 after implant, and treatment started at day 23. The tumor size was evaluated twice weekly, and the tumor volume was measured as (length × width/2)/2 until dosed for 21 days.

Immunohistochemistry and immunofluorescence

All of the tissues were fixed in 10% neutral formalin and embedded in paraffin. Then, 4-μm thick sections were mounted on slides, deparaffinized and rehydrated. After antigen retrieval, slides were blocked in a 3% H_2O_2 solution.

For the immunohistochemical straining, sections were incubated with primary antibodies (Cell Signaling Technology, USA) overnight at 4 °C and with the corresponding secondary antibody for 1 hour at room temperature the following day. The slides were then incubated with DAB solution and nuclear counterstained with hematoxylin. Finally, sections were examined microscopically.

Immunofluorescence straining was performed similarly to the above description. For the nuclear counterstain, slides were counterstained with 4′, 6-diamidino-2-phenylindole dihydrochloride hydrate (DAPI). All images were obtained using a fluorescence microscope.

Mammosphere formation assay

A mammosphere formation assay was conducted using serum-free medium DMEM/F12 (Gibco, Grand Island, USA) supplemented with B27 (Gibco, Grand Island, USA), 20 ng/mL EGF, 20 ng/mL bFGF(Sino Biological Inc., Beijing, China), 4 mg/mL insulin (Gibco, Grand Island, USA), 100 U/mL penicillin and 100 U/mL streptomycin as described earlier [25,37]. In the MCF-7 models, tumors tissues were minced into small pieces and processed with collagenase for 2 hours at 37 °C. After centrifugation, the cell pellet was further trypsinized and passed through an 80-μm filter to produce a single-cell suspension. Dissociated tumor cells were seeded into a 6-well ultralow attachment plate for mammosphere formation. After being cultured for 1–2 weeks, mammospheres with diameter >60 μm were counted under an OLYMPUS inverted microscope.

Flow cytometry analysis of surface markers CD44 and CD24

Signal cells from treated tumors were collected as described above. After blocking, the cells were stained with stem cell markers and analyzed by flow cytometry using a BD FACSCalibur flow cytometer (BD Biosciences, USA). All of the antibodies for the cell surface markers were obtained from Miltenyi Biotec, including phycoerythrin (PE) anti-human CD44 and allophycocyanin anti-human CD24.

Statistical analysis

Data are indicated as means ± SD. Statistical analyses were estimated using the student's *t* test and $P \leq 0.05$ was considered a statistically significant difference between experimental groups. The calculation was performed with the GraphPad Prism software.

Results

Generation of mouse anti-DLL4 monoclonal antibody

After the impact immunization, the mouse with the highest serum antibody titer yielded a serum titer of 1:200,000 (Fig. 1A). The selected positive hybridoma subclone named MMGZ01 was expanded for producing mAbs against rhDLL4. High concentration MMGZ01 was prepared from the ascites of BALB/C mice and purified by Protein A affinity chromatography. By SDS-PAGE detection,

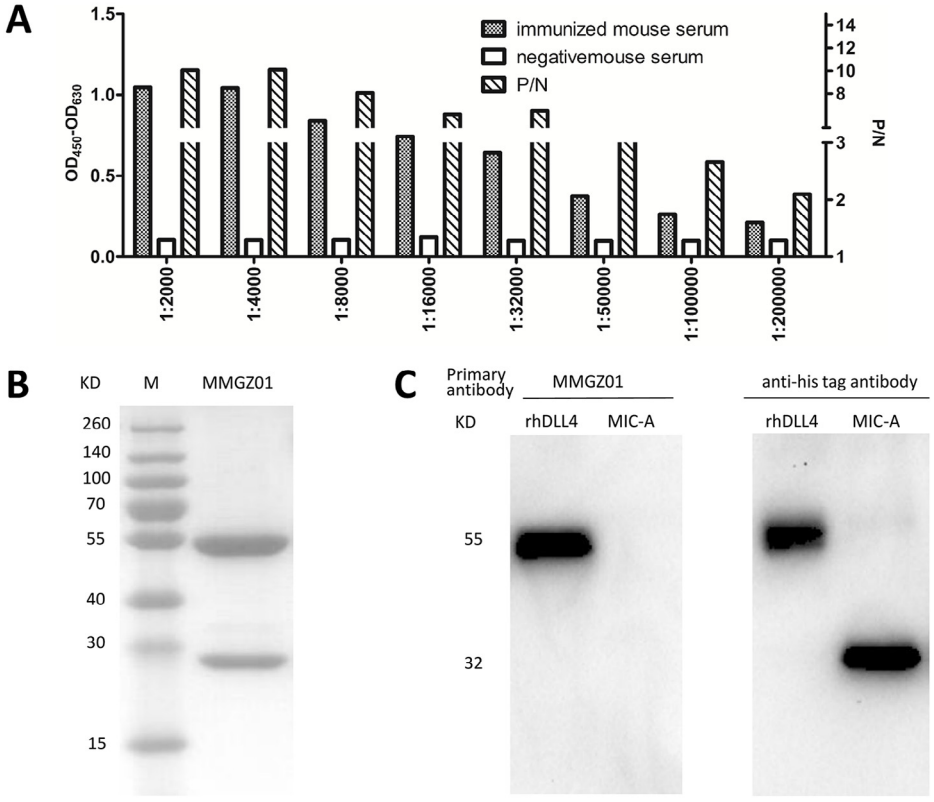

Fig. 1. Generation and characterization of MMGZ01. (A) The serum titer of the mouse after the impact immunization was measured by indirect ELISA. The mouse with serum titer reaching 1:200,000 was selected. (B) SDS-PAGE analysis for the purification of MMGZ01 in reducing condition. (C) Western blot assay of his-tagged rhDLL4 or his-tagged MIC-A detected by MMGZ01. MMGZ01 specifically detected the rhDLL4 but not the unrelated recombinant protein MIC-A, which was detected by rabbit anti-his antibody.

the purified antibody appeared as two bands which corresponded to the heavy chain (50 kD) and the light chain (25 kD) of the immunoglobulin, respectively (Fig. 1B). The heavy chain of MMGZ01 was determined to be IgG2a isotype and the light chain was κ isotype using the isotyping kit (Proteintech Group Inc., China).

Characterization of MMGZ01

A Western blotting assay showed that MMGZ01 and the anti-his tag antibody specifically bind to rhDLL4, whereas MMGZ01 did not detect the MIC-A-his tag that was detected by the anti-his tag antibody (Fig. 1C).

The affinity of MMGZ01 for rhDLL4 was determined using surface plasmon resonance (SPR) spectroscopy, and the kinetic analysis was fitted using a 2:1 binding model. As predicted, the affinity of MMGZ01 with rhDLL4 was measured to be less than 1 pmol/L: (ka (1/Ms): 9.13×10^5, kd (1/s): 3.34×10^{-7}, KD (M): 3.65×10^{-13}) (Fig. 2A and B). These data showed that MMGZ01 exhibited high affinity to rhDLL4.

Compared with the DLL4-negative cell line HEK293, MMGZ01 showed high binding signals with DLL4-expressing HEK293 cells. The binding rates of 200 μg/mL MMGZ01 with DLL4-negative HEK293 and DLL4 expressing HEK293 cells were 1.53% and 74.7%, respectively. The binding rates of control DLL4 mouse mAb with DLL4-negative HEK293 and DLL4 expressing HEK293 cells were 2.75% and 85.3%, respectively (Fig. 2C). The confocal fluorescence microscopy assay revealed that MMGZ01 and control DLL4 mouse mAb showed strong binding signals to DLL4 expressing HEK293 cells,

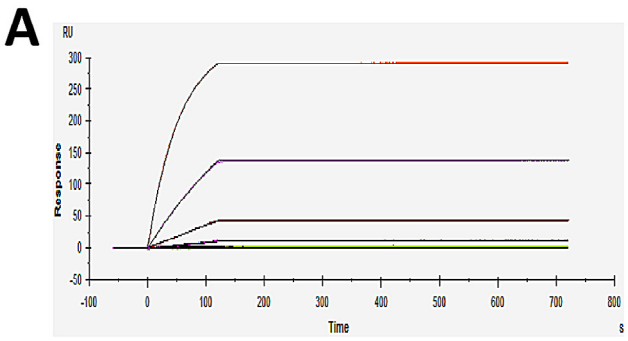

	Ka(1/Ms)	Kd(1/s)	Affinity(KD)
rhDLL4	9.13 e5	3.34 e-7	0.365pM

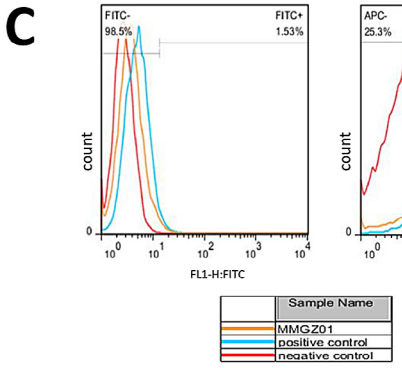

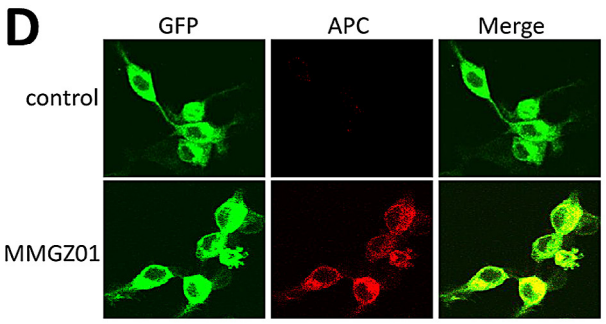

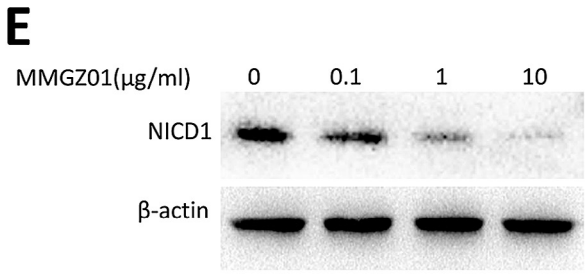

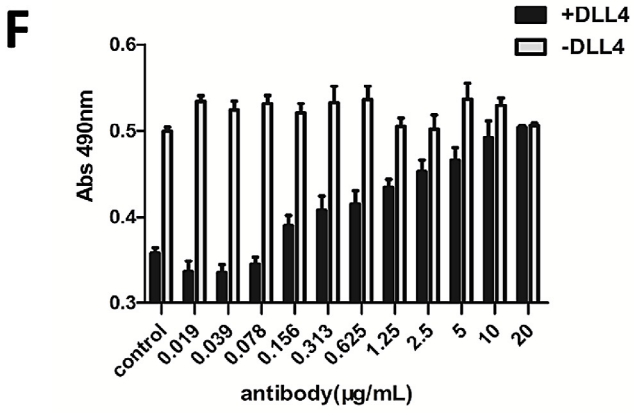

Fig. 2. Specificity analysis of MMGZ01. (A, B) Affinity of MMGZ01 for rhDLL4 was determined by BIAcore. Results for the binding of MMGZ01 to immobilized rhDLL4 showed that the association rate increased with increasing concentration of the MMGZ01. The detailed concentrations of MMGZ01 (from bottom to up) are 0.00125 nM, 0.005 nM, 0.02 nM, 0.078 nM, 0.3125 nM, 1.25 nM, 5 nM and 20 nM. (C) Flow cytometry analysis of the binding of rhDLL4-expressing cells with MMGZ01. HEK293 cells transfected with rhDLL4 (ECD) or a control vector (control) were analyzed using a FACSCalibur flow cytometer. The cells were incubated with a mouse anti-rhDLL4 antibody (positive control) or MMGZ01 and an APC-labeled secondary antibody. (D) Characterization of MMGZ01 by immunofluorescent staining of transfected cells. HEK293 cells transfected with rhDLL4 (ECD) were subsequently fixed and stained immunofluorescently with or without MMGZ01. Green: GFP; Red: APC. (E) MMGZ01 inhibits DLL4-mediated cleavage of the Notch1 receptor. HUVECs were seeded into a 6 well culture plate which has been coated with 1 μg/mL of rhDLL4 for 4 hours, then 0.1, 1 and 10 μg/mL of MMGZ01 or vehicle control were added and cultured for 24 hours. Western blot analysis of Notch1 cleavage was conducted by an antibody to cleaved Notch1 (Val1744). β-actin protein was used as control. (F) MMGZ01 blocks DLL4-mediated inhibition of HUVEC proliferation. HUVECs growing on a 96-well plate pre-coated with 1 μg/mL of rhDLL4 protein were treated with different concentration of MMGZ01 or vehicle control for 96 hours. (For interpretation of the references to color in this figure legend, the reader is referred to the web version of this article.)

whereas few signals were detected between the MMGZ01 and DLL4-negative cell line HEK293 (Fig. 2D). These results indicated that MMGZ01 efficiently binds to DLL4 in a cellular context.

MMGZ01 inhibits endothelial cell Notch1 cleavage and blocks DLL4-mediated inhibition of HUVEC proliferation

Based on current research, interactions between DLL4 and Notch1 would induce cleavage of the receptor [38]. To assess the inhibition of MMGZ01 on cleavage of the Notch1 receptor, sample-treated HUVEC extracts were harvested for Western blotting. Compared with the vehicle control, MMGZ01 dose-dependently inhibited the cleavage of Notch1 by anti-cleaved Notch1 (Val1744). This result demonstrated that MMGZ01 effectively blocked the DLL4-induced cleavage of endogenous Notch1 expressed on HUVECs (Fig. 2E).

The HUVEC proliferation assay revealed that rhDLL4 alone inhibits cell proliferation compared to the control group. After adding different concentrations of MMGZ01, the inhibition of HUVEC proliferation induced by rhDLL4 was significantly alleviated. When the concentration of MMGZ01 reached 20 μg/mL, the suppression of HUVEC proliferation by rhDLL4 was completely reversed (Fig. 2F). These data indicate that MMGZ01 might be responsible for the inhibition of HUVEC proliferation induced by rhDLL4.

MMGZ01 induces sprouting and tube formation

To explore the function of MMGZ01 on the HUVEC phenotype in vitro, a vessel sprouting model was applied to investigate if MMGZ01 could promote HUVEC outward migration. Consistent with our HUVEC proliferation data, we found that MMGZ01 exhibited enhanced angiogenic behavior in a dose-dependent manner in the presence of VEGF relative to control, and bevacizumab results in reduced sprouting (Fig. 3A and B).

Similarly to the tube formation assay, HUVEC tube formation induced by MMGZ01 was dramatically increased compared to control, and bevacizumab inhibited capillary tube formation in the presence of VEGF (Fig. 3C and D). These data are consistent with recognized researches showing that blocking the DLL4-Notch1 signaling pathway leads to increased angiogenesis [20,39].

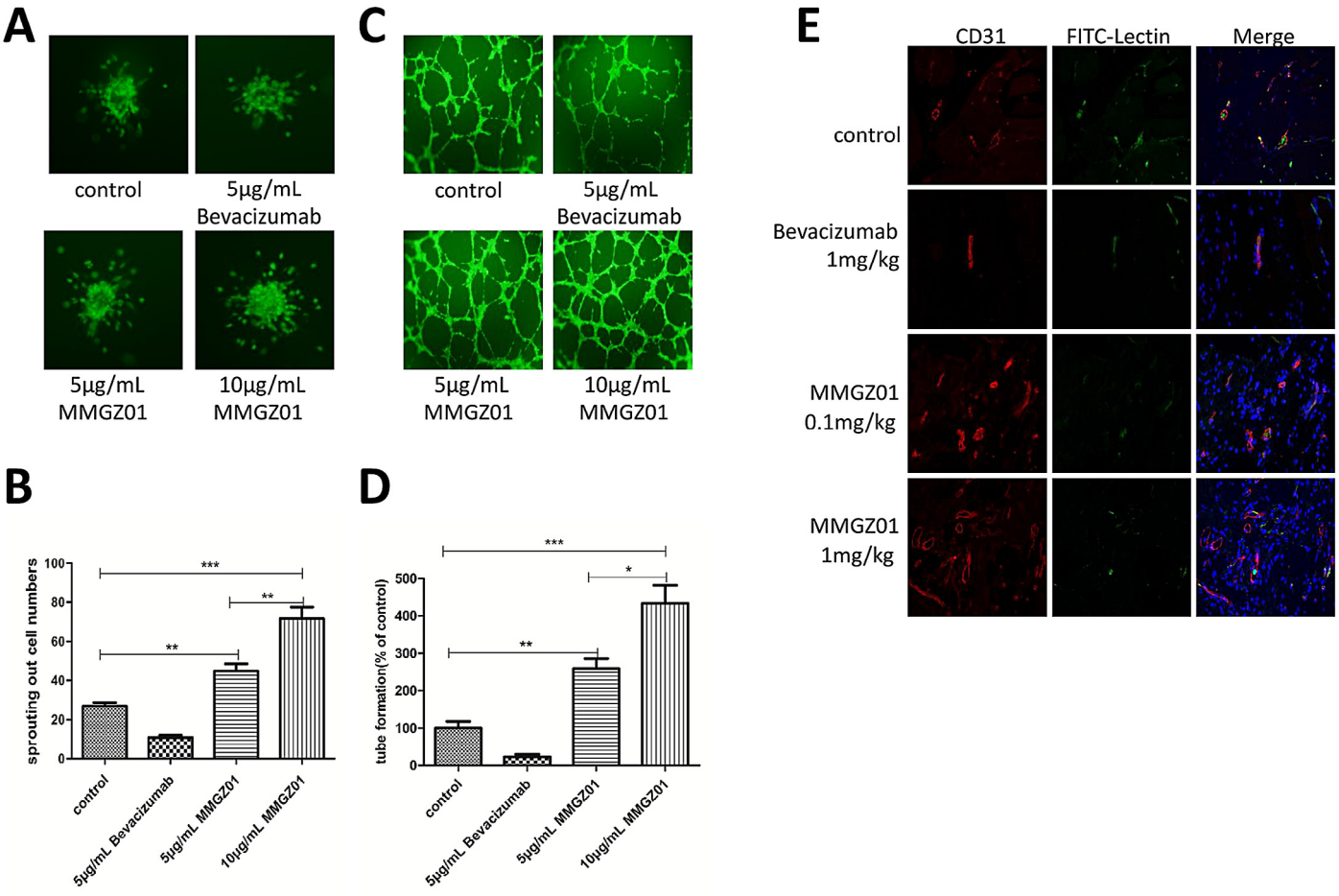

Fig. 3. MMGZ01 induces HUVEC angiogenesis in vitro and in vitro. (A) Photomicrographs of the vessel sprouting assay indicated that MMGZ01 induces sprouting in HUVEC spheroids in vitro. Cells migrating away from the calcein AM-labeled HUVEC spheroids into the sprout were counted. (B) Quantitative analyses of the number of HUVECs that migrated away from the spheroids are shown. (C) MMGZ01 induces HUVEC tubule formation in vitro. HUVECs growth on growth factor reduced Matrigel with vehicle control, 5 μg/mL bevacizumab, 5 or 10 μg/mL MMGZ01 for 4–16 hours. (D) Statistical analysis of the number of complete tubes in treated HUVECs. (E) MMGZ01 induces vessel response with poor perfusion in an in vivo Matrigel plug assay. Mice were dosed every 3 days with vehicle control, 1 mg/kg bevacizumab, 0.1 or 1 mg/kg MMGZ01 until day 21. Vascular perfusion was determined by injecting fluorescein isothiocyanate (FITC)-conjugated lectin (green) intravenously 30 minutes prior to harvesting plugs. Lectin was localized to perfused areas (green), and blood vessels were indicated with CD31 staining (red). Data are presented as the mean ± SD, n = 5 (B, D), $^{*}p < 0.05$, $^{**}p < 0.01$, $^{***}p < 0.001$, NS, no significance. (For interpretation of the references to color in this figure legend, the reader is referred to the web version of this article.)

MMGZ01 induces deficient vessel perfusion of Matrigel plugs in vivo

A human endothelial cell Matrigel plug model was performed to explore how MMGZ01 modulate angiogenesis in vivo. A HUVEC spheroids–Matrigel mixture containing VEGF and FGF-2 was re-suspended with human endothelial cells and subcutaneously injected into 6-week-old BALB/C nude mice [35]. Beginning the next day, the mice were treated intravenously with vehicle control, 1 mg/kg bevacizumab, 0.1 or 1 mg/kg MMGZ01 every 2 days for a total of 21 days. To evaluate vascular perfusion, the mice were intravenously injected with fluorescent isothiocyanate (FITC)-conjugated lectin (Sigma-Aldrich, St. Louis/MO, USA) and were sacrificed 30 minutes later [19,36]. The immunofluorescence examination with CD31 demonstrated that plugs treated with MMGZ01 resulted in a marked increase in vascular structures and a reduction in functional vascularization, whereas bevacizumab treatment group only showed reduced vascular structures relative to control (Fig. 3E).

Effect of MMGZ01 treatment on tumor growth, angiogenesis, proliferation, and apoptosis

To evaluate the efficacy of MMGZ01 in a breast tumor cell line, BALB/C nude mice were xenografted with MDA-MB-231 and MCF-7 tumors. Tumor bearing mice were treated with vehicle control, 10 mg/kg docetaxel, 5 mg/kg MMGZ01 and a combination of 5 mg/kg MMGZ01 + 10 mg/kg docetaxel intravenously every 3 days. Compared with control, the inhibitory rates of MDA-MB-231 tumor growth in animals treated with 10 mg/kg docetaxel, 5 mg/kg MMGZ01 and 5 mg/kg MMGZ01 + 10 mg/kg docetaxel were 44.2%, 56.5% and 77.5% (Fig. 4A and C). The same effects were observed in MCF-7 tumor xenografts. Treatment of mice with docetaxel at 10 mg/kg resulted in a 50.4% decrease in tumor volume compared with PBS, treatment with MMGZ01 at 5 mg/kg resulted in a 41.0% decrease, and combination treatment resulted in an additive effect with 73.6% inhibition (Fig. 4B and D).

Further analysis of the IHC results revealed that MMGZ01-treated MDA-MB-231 tumors exhibited decreased Ki-67 expression and increased cleaved-caspase3. The combination treatment resulted in a pronounced reduction of Ki67, whereas either single agent treated alone caused a moderate decrease in tumor growth (Fig. 5A). These results are consistent with the antitumor effect of tumor growth inhibition. Tumor sections stained with cleaved-caspase 3 for apoptosis showed that the combination treatment caused higher levels of cleaved-caspase 3 than either single agent alone (Fig. 5B).

Furthermore, tumors treated with MMGZ01 or the combination of MMGZ01 and docetaxel showed more neoangiogenic vessels, whereas the percentage of smooth muscle actin (SMA)-positive mural cells, which was measured by CD31 antibody and α-smooth

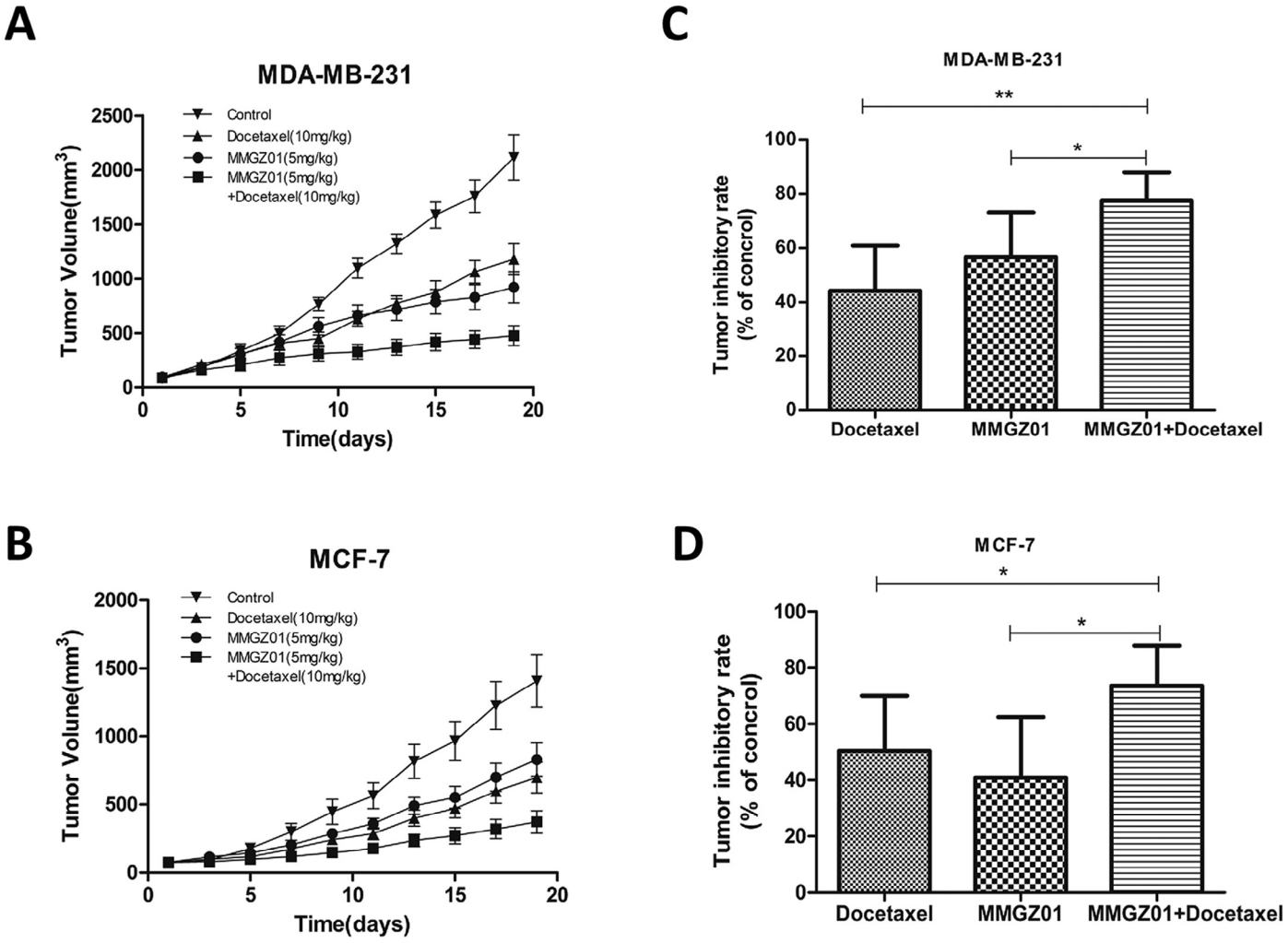

Fig. 4. MMGZ01 enhances docetaxel efficacy in breast cancer models. (A, B) MDA-MB-231 and MCF-7 tumor growth curves for nude mice. Mice were injected subcutaneously with MDA-MB-231 or MCF-7 cells (5×10^6) and grouped before treatment began. Tumor volume was measured using vernier calipers following tumor development. (C) (D) Tumor inhibition rates of different dosage groups. Data are presented as the mean ± SD, n = 6, $^*p < 0.05$, $^{**}p < 0.01$.

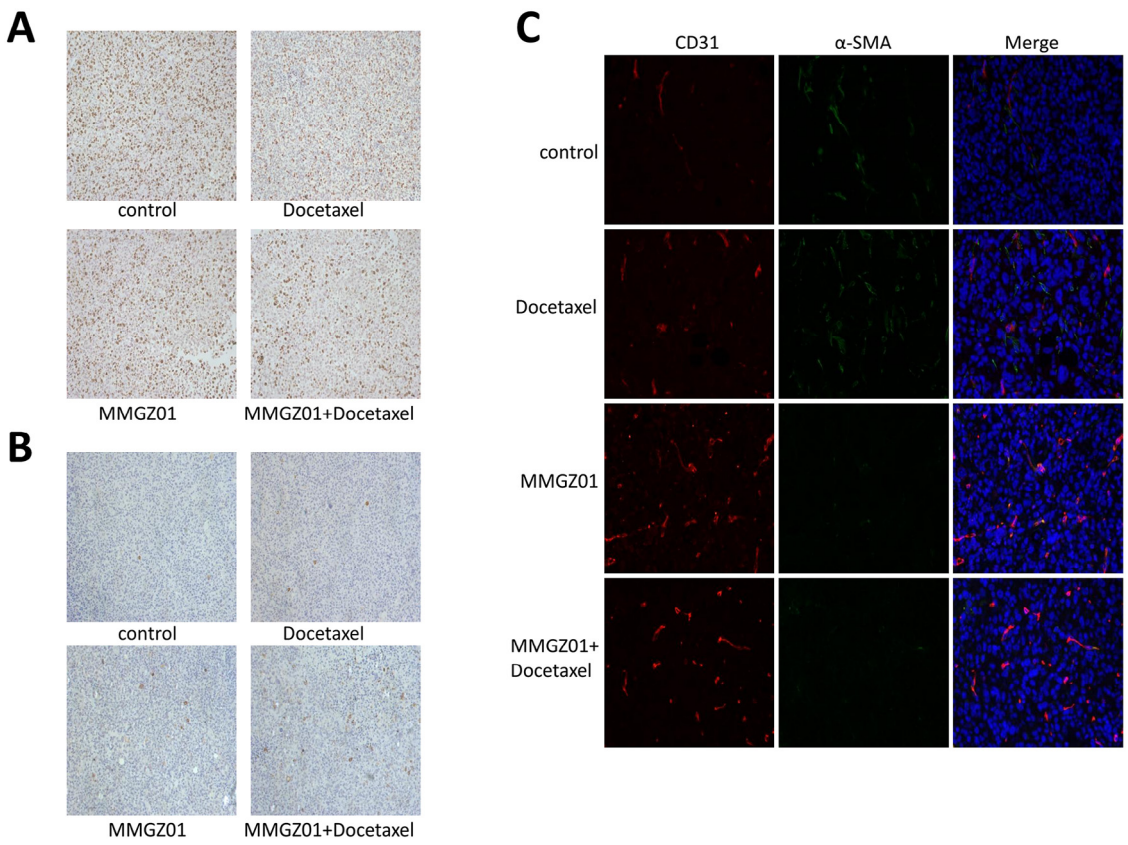

Fig. 5. MMGZ01 combined with docetaxel inhibits cell proliferation, induces apoptosis and promotes non-productive angiogenesis in MDA-MB-231 tumors. (A) IHC staining of Ki-67 (anti-Ki 67 antibody) for proliferation in paraffin sections of xenografted tumor. (B) IHC staining of cleaved-caspase 3 (anti-cleaved caspase 3) for apoptosis in paraffin sections of xenografted tumor. (C) Tumor vessel number and perfusion were determined by an antibody to SMA (green) for mural cells and a CD31 antibody (red) for vessel staining. (For interpretation of the references to color in this figure legend, the reader is referred to the web version of this article.)

muscle actin antibody, was decreased. Tumors treated with vehicle control or docetaxel alone showed fewer vessels, and the portion of effective vessels was not reduced (Fig. 5C).

MMGZ01 depletes subpopulation of putative breast cancer stem-like cells, leading to the reversal of the epithelial-to-mesenchymal transition

To investigate the effect of MMGZ01 on the population of breast cancer stem-like cells, MCF-7 tumor cells were isolated and the expression levels of the stem cell markers CD44 and CD24 were examined using flow cytometry. The flow cytometric analysis showed a moderate increase in the $CD44^{+}/CD24^{-}$ subpopulation in the docetaxel treatment group, whereas there was a significant decrease in the MMGZ01 treatment groups (Fig. 6A).

Mammosphere formation assay was also utilized to evaluate the self-renew capacity of cancer cells. To quantify the mammosphere formation from different treatment groups, 1×10^4 single cells were seeded in suspension culture in 6-well ultralow attachment plates. After being cultured for 1–2 weeks, the numbers of formed mammospheres (>60 μm) were recorded. The results showed a marked increase in mammosphere formation in the docetaxel treatment group and a significant reduction in the MMGZ01 treatment group (Fig. 6B and C).

EMT is involved in tumor progression, metastasis, and stem cell-like characteristics in many tumors, including breast cancer [23,37,40]. Evidence shows that Notch pathway activation plays a critical role in the acquisition of EMT [41,42]. We examined the expression of EMT markers including Snail, E-cadherin, and Slug. The Western blot analysis revealed that treatment with docetaxel increased the expression level of Snail and Slug, whereas there was decreased epithelial-associated gene E-cadherin compared with control. MMGZ01 treatment reversed the docetaxel-induced increase in the expression of Snail and Slug in the tumor cells and increased E-cadherin expression in the tumor cells (Fig. 6D). Our findings strongly suggest that MMGZ01 treatment induced the reversal of EMT.

Discussion

Angiogenesis plays a critical role in promoting tumor angiogenesis and metastasis. The formation of a vascular network requires a specific factors within spatiotemporal constraints to stimulate and construct the vascular system [43]. DLL4 is a constituent expressed in human arterial endothelial cells and is induced by the VEGF/VEGFR2 pathway. Recent studies have suggested that the DLL4-Notch signaling pathway acts as a negative regulator of vascular morphogenesis and remodeling, and the blockade of DLL4 in tumors could induce excessive vessels with limited perfusion, consequently preventing tumor growth [19,44,45].

In this study, a novel human DLL4-specific monoclonal antibody was prepared through hybridoma technology. The affinity of MMGZ01 with rhDLL4 was measured to be less than 1 pmol/L, which was the highest compared to other anti-DLL4 antibodies reported. Beyond that, comprehensive evaluations in vitro and in vivo revealed that MMGZ01 effectively inhibits the binding of DLL4 to Notch1 and modulates HUVEC function. In addition to the effect on deregulating angiogenesis in the vasculature, our study for the first time demonstrated that using MMGZ01 to target DLL4-Notch signaling results in anti-tumor effects through multiple mechanisms

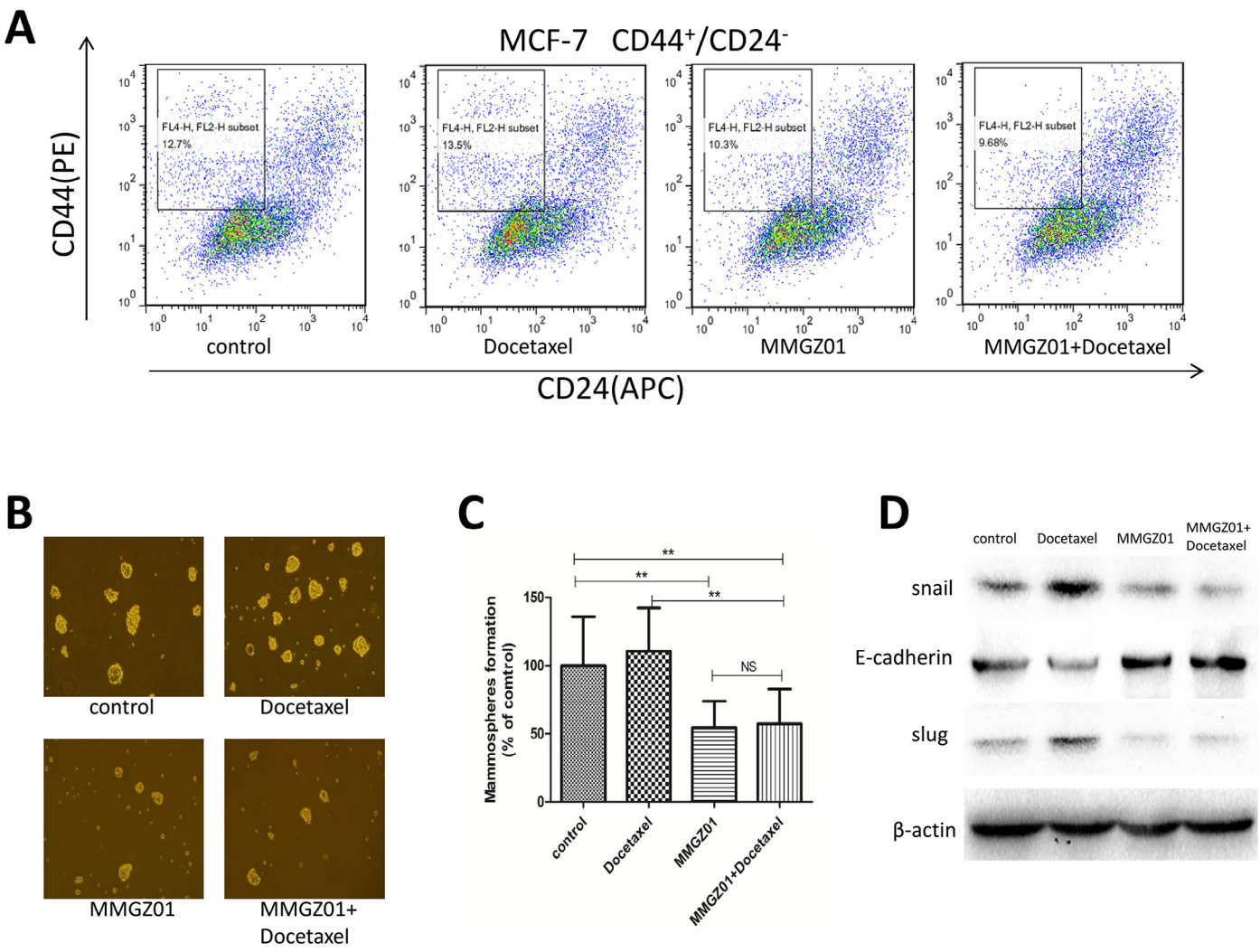

Fig. 6. MMGZ01 enhances docetaxel efficacy in MCF-7 tumors by reducing mammosphere formation, decreasing $CD44^+/CD24^-$ population and modulating EMT marker expression. (A) Tumors from each group were dissociated into single-cell suspensions. Expression of cell surface markers CD44 and CD24 was examined by flow cytometry using specific antibodies. (B) 1×10^4 single cells isolated from MCF-7 xenografts were cultured in low attachment 6 well culture plates for 1–2 weeks to form the mammospheres. (C) Quantitation of the mammosphere-forming efficiency. The numbers of mammospheres (>60 μm) were recorded after 1–2 weeks of culture. Data are presented as the mean ± SD, n = 9, $^*p < 0.05$, $^{**}p < 0.01$, NS, no significance. (D) Effect of MMGZ01 and docetaxel on EMT marker expression. β-actin protein was used as a loading control.

when administered with docetaxel and enhances the docetaxel-mediated cytotoxicity against MDA-MB-231 and MCF-7 xenograft tumors. We demonstrated that the MMGZ01 meditated anti-tumor effect occurred through the inhibition of tumor cell proliferation and through the promotion of tumor cell apoptosis in MDA-MB-231 xenografte tumors. MMGZ01 was shown to decrease the cancer stem-like cell population, leading to the reversal of the epithelial-to-mesenchymal transition in MCF-7 xenograft tumors. These results revealed potential mechanisms on how DLL4 blockade meditates its activity in breast cancer, and indicated that targeting DLL4-Notch signaling might be an effective therapeutic strategy for breast cancer patients in combination with docetaxel.

Evidence suggests that Notch families are majorly expressed in the vasculature and that dysfunctional vascular phenotypes are associated with aberrations in normal Notch signaling [10,46]. To assess the effect of MMGZ01 on endothelial cell function in vitro, endothelial cell spheroid sprouting and endothelial cell tube formation assays were performed. Enhanced endothelial spheroid sprouting was detected with VEGF and MMGZ01 administration. The HUVEC tube formation assay showed that increased tube formation was induced with the addition of either VEGF or MMGZ01. These data suggest that MMGZ01 was able to induce endothelial cell tube formation and sprouting, which is consistent with the accepted findings that DLL4 is a negative regulator of angiogenesis.

The complexity of angiogenesis limits the methods of anti-angiogenic studies [11,47]. A Matrigel plug angiogenesis assay, equipped with simplicity and robustness, was performed to evaluate the stimulation of vascular remodeling [36]. MMGZ01 was observed to induce abundant microvessels with rare red blood cells in a dose-dependent manner; these results differed from bevacizumab treatment, as determined by detection of both CD31 positive and FITC-lectin positive endothelial cells. These results suggest that the combination of anti-DLL4 and bevacizumab is a promising anti-angiogenesis therapeutic strategy for tumors. Similar to our results, recent studies in an EL4 mouse lymphoma tumor model report that the blockade of DLL4-Notch signaling using DBZ, a small molecule inhibitor of γ-secretase, or a humanized phage anti-DLL4 antibody is associated with a marked reduction in normal tumor vessels [19]. In contrast to inhibiting the Notch pathway through γ-secretase inhibitors by blocking all Notch receptors activities, which might induce potential side effects such as gastrointestinal toxicity, the DLL4 blockade could achieve the therapeutic

aim more safely and effectively. The characteristics of destruction in the tumor vasculature and blood vessel perfusion suggest that further studies should focus on the fate of this abnormal neovasculature [48].

In addition to the effect on angiogenesis by targeting DLL4 in the vasculature, the tumor growth inhibition assay showed that MMGZ01, alone or in combination with docetaxel, exhibited a remarkable anti-tumor effect, reducing MDA-MB-231 and MCF-7 tumor growth. The survival time of tumor-bearing nude mice was also significantly prolonged. MMGZ01 was found to induce excessive but dysfunctional blood vessel formation compared with the control or docetaxel treatment. The murine derived monoclonal antibodies could trigger a HAMA response, resulting in increased toxicity and shortened half-life in patients [49,50]. Therefore, the development of our monoclonal antibody would be worthwhile in the targeting of tumor vasculature in humans.

Accumulating evidence demonstrates that the inhibition of Notch signaling reduces the number of cancer stem cells, indicating the critical role of Notch signaling in the maintenance of the cancer stem cell phenotype [23,41]. Recently, Ming Qiu et al. demonstrated that a Notch1 targeted antibody, either alone or in combination with the chemotherapeutic agent docetaxel, reduced triple negative breast cancer stem cells [25]. Our results showed that blockade of DLL4 leads to tumor growth inhibition through various mechanisms, in part, because the effects of EMT features, mammosphere formation and $CD44^{+}/CD24^{-}$ subpopulation, which are important characteristics of the putative cancer stem-like cell subpopulation in breast cancers, were effectively inhibited by MMGZ01, either alone or in combination with docetaxel. These results implied that our antibody is capable of suppressing putative breast cancer stem cell-like characteristics. Both studies suggest a vital function of DLL4-Notch signaling in breast CSC activity. Although the role of Notch signaling in CSC has been widely investigated, the relationship between DLL4-Notch signaling and the CSC phenotype remains unclear.

We described the discovery of the DLL4 targeted monoclonal antibody MMGZ01 and provided experimental data to explore the mechanism of MMGZ01 in halting breast tumor growth and regulating angiogenesis and vessel maturation in vitro and in vivo. These findings indicated that anti-DLL4 acts as a potential treatment for breast cancer through multiple mechanisms. Taken together, the findings provide support for developing our anti-DLL4-neutralizing agents further as single agents or in combination with chemotherapy to improve treatment outcomes for patients with breast cancer.

Acknowledgements

This work was supported by the National Natural Science Foundation of China (NSFC81102364, NSFC81273425 and NSFC81473125), the Natural Science Foundation of Jiangsu Province (Grants No BK20140675), the Fundamental Research Funds for the Central Universities (JKY2011025), the Project Program of State Key Laboratory of Natural Medicines (China Pharmaceutical University, JKGP201101), and a project funded by the Priority Academic Program Development of Jiangsu Higher Education Institutions.

Conflict of interest

The authors declare that they have no conflicts of interest.

Appendix: Supplementary material

Supplementary data to this article can be found online at doi:10.1016/j.canlet.2015.12.025.

References

[1] J. Baselga, M. Campone, M. Piccart, H.A. Burris 3rd, H.S. Rugo, T. Sahmoud, et al., Everolimus in postmenopausal hormone-receptor-positive advanced breast cancer, N. Engl. J. Med. 366 (2012) 520–529.
[2] J.-Q. Chen, J. Russo, ERα-negative and triple negative breast cancer: molecular features and potential therapeutic approaches, Biochim. Biophys. Acta 1796 (2009) 162–175.
[3] S. Aliwaini, J. Peres, W.L. Kröger, A. Blanckenberg, J. de la Mare, A.L. Edkins, et al., The palladacycle, AJ-5, exhibits anti-tumour and anti-cancer stem cell activity in breast cancer cells, Cancer Lett. 357 (2015) 206–218.
[4] F. Al-Ejeh, C.E. Smart, B.J. Morrison, G. Chenevix-Trench, J.A. Lopez, S.R. Lakhani, et al., Breast cancer stem cells: treatment resistance and therapeutic opportunities, Carcinogenesis 32 (2011) 650–658.
[5] E.Y. Park, E. Chang, E.J. Lee, H.W. Lee, H.G. Kang, K.H. Chun, et al., Targeting of miR34a-NOTCH1 axis reduced breast cancer stemness and chemoresistance, Cancer Res. 74 (2014) 7573–7582.
[6] J.R. Shutter, S. Scully, W. Fan, W.G. Richards, J. Kitajewski, G.A. Deblandre, et al., Dll4, a novel Notch ligand expressed in arterial endothelium, Genes Dev. 14 (2000) 1313–1318.
[7] R. Kopan, M.X. Ilagan, The canonical Notch signaling pathway: unfolding the activation mechanism, Cell 137 (2009) 216–233.
[8] C. Mailhos, U. Modlich, J. Lewis, A. Harris, R. Bicknell, D. Ish-Horowicz, Delta4, an endothelial specific notch ligand expressed at sites of physiological and tumor angiogenesis, Differentiation 69 (2001) 135–144.
[9] S.J. Bray, Notch signalling: a simple pathway becomes complex, Nat. Rev. Mol. Cell Biol. 7 (2006) 678–689.
[10] N.M. Kofler, C.J. Shawber, T. Kangsamaksin, H.O. Reed, J. Galatioto, J. Kitajewski, Notch signaling in developmental and tumor angiogenesis, Genes Cancer 2 (2011) 1106–1116.
[11] L.K. Phng, H. Gerhardt, Angiogenesis: a team effort coordinated by notch, Dev. Cell 16 (2009) 196–208.
[12] N.W. Gale, M.G. Dominguez, I. Noguera, L. Pan, V. Hughes, D.M. Valenzuela, et al., Haploinsufficiency of delta-like 4 ligand results in embryonic lethality due to major defects in arterial and vascular development, Proc. Natl. Acad. Sci. U.S.A. 101 (2004) 15949–15954.
[13] A.M. Jubb, E.J. Soilleux, H. Turley, G. Steers, A. Parker, I. Low, et al., Expression of vascular notch ligand delta-like 4 and inflammatory markers in breast cancer, Am. J. Pathol. 176 (2010) 2019–2028.
[14] S. Indraccolo, S. Minuzzo, M. Masiero, I. Pusceddu, L. Persano, L. Moserle, et al., Cross-talk between tumor and endothelial cells involving the Notch3-Dll4 interaction marks escape from tumor dormancy, Cancer Res. 69 (2009) 1314–1323.
[15] N. El Hindy, K. Keyvani, A. Pagenstecher, P. Dammann, I.E. Sandalcioglu, U. Sure, et al., Implications of Dll4-Notch signaling activation in primary glioblastoma multiforme, Neuro Oncol. 15 (2013) 1366–1378.
[16] M.E. Mullendore, J.B. Koorstra, Y.M. Li, G.J. Offerhaus, X. Fan, C.M. Henderson, et al., Ligand-dependent Notch signaling is involved in tumor initiation and tumor maintenance in pancreatic cancer, Clin. Cancer Res. 15 (2009) 2291–2301.
[17] S. Ishigami, T. Arigami, Y. Uenosono, H. Okumura, H. Kurahara, Y. Uchikado, et al., Clinical implications of DLL4 expression in gastric cancer, J. Exp. Clin. Cancer Res. 32 (2013) 46.
[18] N.S. Patel, M.S. Dobbie, M. Rochester, G. Steers, R. Poulsom, K. Le Monnier, et al., Up-regulation of endothelial delta-like 4 expression correlates with vessel maturation in bladder cancer, Clin. Cancer Res. 12 (2006) 4836–4844.
[19] J. Ridgway, G. Zhang, Y. Wu, S. Stawicki, W.C. Liang, Y. Chanthery, et al., Inhibition of Dll4 signalling inhibits tumour growth by deregulating angiogenesis, Nature 444 (2006) 1083–1087.
[20] I. Noguera-Troise, C. Daly, N.J. Papadopoulos, S. Coetzee, P. Boland, N.W. Gale, et al., Blockade of Dll4 inhibits tumour growth by promoting non-productive angiogenesis, Nature 444 (2006) 1032–1037.
[21] H. Harrison, G. Farnie, S.J. Howell, R.E. Rock, S. Stylianou, K.R. Brennan, et al., Regulation of breast cancer stem cell activity by signaling through the Notch4 receptor, Cancer Res. 70 (2010) 709–718.
[22] S. Guo, M. Liu, R.R. Gonzalez-Perez, Role of Notch and its oncogenic signaling crosstalk in breast cancer, Biochim. Biophys. Acta 1815 (2011) 197–213.
[23] W. Zhou, G. Wang, S. Guo, Regulation of angiogenesis via Notch signaling in breast cancer and cancer stem cells, Biochim. Biophys. Acta 2013 (1836) 304–320.
[24] E. Charafe-Jauffret, C. Ginestier, F. Iovino, J. Wicinski, N. Cervera, P. Finetti, et al., Breast cancer cell lines contain functional cancer stem cells with metastatic capacity and a distinct molecular signature, Cancer Res. 69 (2009) 1302–1313.
[25] M. Qiu, Q. Peng, I. Jiang, C. Carroll, G. Han, I. Rymer, et al., Specific inhibition of Notch1 signaling enhances the antitumor efficacy of chemotherapy in triple negative breast cancer through reduction of cancer stem cells, Cancer Lett. 328 (2013) 261–270.
[26] G. Farnie, R.B. Clarke, Mammary stem cells and breast cancer – role of notch signalling, Stem Cell Rev. 3 (2007) 169–175.
[27] H. He, X. Tu, J. Zhang, D.O. Acheampong, L. Ding, Z. Ma, et al., A novel antibody targeting CD24 and hepatocellular carcinoma in vivo by near-infrared fluorescence imaging, Immunobiology 220 (2015) 1328–1336.
[28] W. Xie, D. Li, J. Zhang, Z. Li, D.O. Acheampong, Y. He, et al., Generation and characterization of a novel human IgG1 antibody against vascular endothelial growth factor receptor 2, Cancer Immunol. Immunother. 63 (2014) 877–888.

[29] Y. Zhou, Y.D. Fan, L.B. Zeng, Construction of a recombinant eukaryotic vector for a grass carp reovirus VP6 gene and its expression in vitro and in vivo, Virusdisease 25 (2014) 69–77.
[30] C.C. Zhang, Z. Yan, Q. Zong, D.D. Fang, C. Painter, Q. Zhang, et al., Synergistic effect of the gamma-secretase inhibitor PF-03084014 and docetaxel in breast cancer models, Stem Cells Transl. Med. 2 (2013) 233–242.
[31] I. Arnaoutova, H.K. Kleinman, In vitro angiogenesis: endothelial cell tube formation on gelled basement membrane extract, Nat. Protoc. 5 (2010) 628–635.
[32] T. Korff, H.G. Augustin, Tensional forces in fibrillar extracellular matrices control directional capillary sprouting, J. Cell Sci. 112 (Pt 19) (1999) 3249–3258.
[33] T. Korff, H.G. Augustin, Integration of endothelial cells in multicellular spheroids prevents apoptosis and induces differentiation.pdf, J. Cell Biol. 143 (1998) 1341–1352.
[34] Q. Jiang, M. Lagos-Quintana, D. Liu, Y. Shi, C. Helker, W. Herzog, et al., miR-30a regulates endothelial tip cell formation and arteriolar branching, Hypertension 62 (2013) 592–598.
[35] J. Kendrew, C. Eberlein, B. Hedberg, K. McDaid, N.R. Smith, H.M. Weir, et al., An antibody targeted to VEGFR-2 Ig domains 4-7 inhibits VEGFR-2 activation and VEGFR-2-dependent angiogenesis without affecting ligand binding, Mol. Cancer Ther. 10 (2011) 770–783.
[36] A.M. Laib, A. Bartol, A. Alajati, T. Korff, H. Weber, H.G. Augustin, Spheroid-based human endothelial cell microvessel formation in vivo, Nat. Protoc. 4 (2009) 1202–1215.
[37] A. Sharma, A.N. Paranjape, A. Rangarajan, R.R. Dighe, A monoclonal antibody against human Notch1 ligand-binding domain depletes subpopulation of putative breast cancer stem-like cells, Mol. Cancer Ther. 11 (2012) 77–86.
[38] E.H. Schroeter, J.A. Kisslinger, R. Kopan, Notch-1 signalling requires ligand-induced proteolytic release of intracellular domain, Nature 393 (1998) 382–386.
[39] D.W. Jenkins, S. Ross, M. Veldman-Jones, I.N. Foltz, B.C. Clavette, K. Manchulenko, et al., MEDI0639: a novel therapeutic antibody targeting Dll4 modulates endothelial cell function and angiogenesis in vivo, Mol. Cancer Ther. 11 (2012) 1650–1660.
[40] K. Polyak, R.A. Weinberg, Transitions between epithelial and mesenchymal states: acquisition of malignant and stem cell traits, Nat. Rev. Cancer 9 (2009) 265–273.
[41] I. Espinoza, L. Miele, Deadly crosstalk: notch signaling at the intersection of EMT and cancer stem cells, Cancer Lett. 341 (2013) 41–45.
[42] B. Bao, Z. Wang, S. Ali, D. Kong, Y. Li, A. Ahmad, et al., Notch-1 induces epithelial-mesenchymal transition consistent with cancer stem cell phenotype in pancreatic cancer cells, Cancer Lett. 307 (2011) 26–36.
[43] S.M. Weis, D.A. Cheresh, Tumor angiogenesis: molecular pathways and therapeutic targets, Nat. Med. 17 (2011) 1359–1370.
[44] S. Suchting, C. Freitas, F. le Noble, R. Benedito, C. Breant, A. Duarte, et al., The Notch ligand Delta-like 4 negatively regulates endothelial tip cell formation and vessel branching, Proc. Natl. Acad. Sci. U.S.A. 104 (2007) 3225–3230.
[45] I.B. Lobov, E. Cheung, R. Wudali, J. Cao, G. Halasz, Y. Wei, et al., The Dll4/Notch pathway controls postangiogenic blood vessel remodeling and regression by modulating vasoconstriction and blood flow, Blood 117 (2011) 6728–6737.
[46] I.B. Lobov, R.A. Renard, N. Papadopoulos, N.W. Gale, G. Thurston, G.D. Yancopoulos, et al., Delta-like ligand 4 (Dll4) is induced by VEGF as a negative regulator of angiogenic sprouting, Proc. Natl. Acad. Sci. U.S.A. 104 (2007) 3219–3224.
[47] M. Potente, H. Gerhardt, P. Carmeliet, Basic and therapeutic aspects of angiogenesis, Cell 146 (2011) 873–887.
[48] T. Hoey, W.C. Yen, F. Axelrod, J. Basi, L. Donigian, S. Dylla, et al., DLL4 blockade inhibits tumor growth and reduces tumor-initiating cell frequency, Cell Stem Cell 5 (2009) 168–177.
[49] T.T. Hansel, H. Kropshofer, T. Singer, J.A. Mitchell, A.J. George, The safety and side effects of monoclonal antibodies, Nat. Rev. Drug Discov. 9 (2010) 325–338.
[50] J.J. Tjandra, L. Ramadi, I.F. McKenzie, Development of human anti-murine antibody (HAMA) response in patients, Immunol. Cell Biol. 68 (Pt 6) (1990) 367–376.